Sulfide-responsive transcriptional repressor SqrR functions as a master regulator of sulfide-dependent photosynthesis

Takayuki Shimizu[a], Jiangchuan Shen[b,c], Mingxu Fang[c], Yixiang Zhang[b,d], Koichi Hori[e], Jonathan C. Trinidad[b,d], Carl E. Bauer[c], David P. Giedroc[b,c], and Shinji Masuda[f,g,1]

[a]Graduate School of Bioscience and Biotechnology, Tokyo Institute of Technology, Kanagawa 226-8501, Japan; [b]Department of Chemistry, Indiana University, Bloomington, IN 47405-7102; [c]Department of Molecular and Cellular Biochemistry, Indiana University, Bloomington, IN 47405; [d]Laboratory for Biological Mass Spectrometry, Indiana University, Bloomington, IN 47405-7102; [e]School of Life Science and Technology, Tokyo Institute of Technology, Kanagawa 226-8501, Japan; [f]Center for Biological Resources and Informatics, Tokyo Institute of Technology, Kanagawa 226-8501, Japan; and [g]Earth-Life Science Institute, Tokyo Institute of Technology, Tokyo 152-8551, Japan

Sulfide was used as an electron donor early in the evolution of photosynthesis, with many extant photosynthetic bacteria still capable of using sulfur compounds such as hydrogen sulfide (H_2S) as a photosynthetic electron donor. Although enzymes involved in H_2S oxidation have been characterized, mechanisms of regulation of sulfide-dependent photosynthesis have not been elucidated. In this study, we have identified a sulfide-responsive transcriptional repressor, SqrR, that functions as a master regulator of sulfide-dependent gene expression in the purple photosynthetic bacterium *Rhodobacter capsulatus*. SqrR has three cysteine residues, two of which, C41 and C107, are conserved in SqrR homologs from other bacteria. Analysis with liquid chromatography coupled with an electrospray-interface tandem-mass spectrometer reveals that SqrR forms an intramolecular tetrasulfide bond between C41 and C107 when incubated with the sulfur donor glutathione persulfide. SqrR is oxidized in sulfide-stressed cells, and tetrasulfide–cross-linked SqrR binds more weakly to a target promoter relative to unmodified SqrR. C41S and C107S *R. capsulatus* SqrRs lack the ability to respond to sulfide, and constitutively repress target gene expression in cells. These results establish that SqrR is a sensor of H_2S-derived reactive sulfur species that maintain sulfide homeostasis in this photosynthetic bacterium and reveal the mechanism of sulfide-dependent transcriptional derepression of genes involved in sulfide metabolism.

sulfide sensor | photosynthesis regulation | reactive sulfur species | purple bacteria | *Rhodobacter*

The discovery of ~550 deep-sea hydrothermal vents more than 30 y ago (1) has led to the theory that energy metabolism in early ancestral organisms may have arisen from deep-sea hydrothermal vents where simple inorganic molecules such as hydrogen sulfide or hydrogen gas, as well as methane, exist (2–4). Such ancient energy metabolism has been assumed to be similar to that of extant chemolithotrophs, which obtain energy from these molecules. Indeed, various chemolithoautotrophic microbes thrive in deep-sea hydrothermal vents and are capable of oxidizing sulfides, methane, and/or hydrogen gas for use as energy sources and electron donors (5). Some photosynthetic bacteria have also been isolated from deep-sea hydrothermal vents that can grow photosynthetically using sulfide as an electron donor and geothermal radiation as an energy source instead of solar radiation (6), as hypothesized for ancestral phototrophs.

Many purple photosynthetic bacteria have remarkable metabolic versatility required to meet the energy demands of sulfide-dependent and -independent photosynthesis as well as aerobic and anaerobic respiration. These bacteria tightly control the synthesis of their electron transfer proteins involved in each growth mode in response to a specific electron donor, oxygen tension, and light intensity (7, 8). Among these regulatory systems, oxygen- and light-

sensing mechanisms have been well-studied; however, mechanisms used to sense hydrogen sulfide remain incompletely understood.

Understanding the general biological functions of hydrogen sulfide has emerged as a subject of topical interest since its recent description as a gasotransmitter in mammals (9–11). Despite an appreciation of sulfide signaling, the mechanisms of how H_2S functions as a signaling molecule remain under investigation (12). Emerging evidence suggests that highly oxidized sulfur species, termed reactive sulfur species (RSS), are the actual sulfide-signaling species (13–16). These include HS•, cysteine sulfenic acids, cysteine persulfides, glutathione persulfides (GSSHs), and inorganic polysulfide species, which catalyze persulfidation of specific proteins and enzymes (13, 17–20), although the functional impact of this protein modification is as yet not generally clear (17).

Hydrogen sulfide inhibits respiration by poisoning cytochrome oxidase and binding and precipitating biologically required divalent transition metals, and is thus toxic at high concentrations (21). The ability to adapt to a sulfide-rich environment is therefore critical for the survival for some microorganisms. The universal first step in H_2S detoxification and utilization of H_2S as an electron donor

Significance

Hydrogen sulfide is a universal bioactive molecule that functions in both prokaryotes and eukaryotes. However, little is known about intra- and extracellular sulfide-sensing mechanisms. Here we show that the sulfide-regulated repressor SqrR from a purple bacterium forms an intramolecular tetrasulfide bond in response to sulfide stress in vivo and organic persulfides in vitro, revealing the importance of this cysteine modification for sulfide sensing in cells. These findings provide new insights into bacterial sulfide homeostasis and its potential applications in synthetic biology. Given that purple bacteria retain characteristics of ancestral photosynthesis and photosynthetic electron transfer, the functional characterization of SqrR also provides new information on plausible mechanisms that regulated electron flow early in the evolution of photosynthesis.

MICROBIOLOGY

includes the sulfide:cytochrome *c* reductases (SoxF and FccAB) or sulfide:quinone reductases (SQRs), the latter used to reduce quinones via the two-electron oxidation of sulfide to sulfane or zero-valent S^0. In the case of SQRs, S^0 is conjugated to a variety of nucleophilic acceptors, such as sulfite (SO_3^{2-}), CN^-, S^{2-}, or a low-molecular-weight thiol, for example glutathione (22–24), the latter of which gives rise to glutathione persulfide. In the purple photosynthetic bacterium *Rhodobacter capsulatus*, SQR is the major enzyme responsible for catalyzing this first step in sulfide oxidation, with the level of SQR expression increasing after sulfide treatment (25). *R. capsulatus* can also grow photosynthetically, using sulfide as well as several inorganic and organic compounds as electron donors. Thus, *R. capsulatus* seems to use sophisticated regulatory strategies to control different photosynthetic growth modes in response to environmental changes. However, a sulfide-responsive sensor protein has not been identified in *R. capsulatus*.

To better understand sulfide sensing in photosynthetic bacteria, we aimed to identify a sulfide-responsive sensor protein from *R. capsulatus*. Genetic mutant screening resulted in the identification of the transcriptional regulator SqrR, which functions as a repressor of genes responsible for sulfide-dependent photosynthesis. We show that SqrR DNA-binding and transcriptional regulatory activity is regulated by persulfide-dependent cysteine modification, which is analogous to that previously described for the persulfide sensor in *Staphylococcus aureus*, CstR (26). However, SqrR and CstR are derived from distinct structural classes of transcriptional repressors, suggesting that SqrR functions as a novel sensor of sulfide-derived reactive sulfur species in bacterial cells.

Results

Identification of *sqrR* in *R. capsulatus*. To identify a sulfide-regulated sensor protein in photosynthetic bacteria, we took advantage of the well-established genetic system of *R. capsulatus* (27). Because SQR expression in *R. capsulatus* increases upon sulfide treatment (25), we exploited changes in *sqr* expression as a means to isolate sulfide-insensitive mutants. To screen for mutants, we constructed a plasmid where the *sqr* promoter drives *lacZ* expression. To verify whether the *sqr* promoter responds to sulfide specifically, we carried out β-galactosidase assays with *R. capsulatus* containing the *sqr::lacZ* expression plasmid treated with sulfide under aerobic and anaerobic growth conditions. The *sqr* promoter specifically responds to sulfide under both conditions (Fig. 1). Primer extension analysis reveals the presence of a single transcriptional start site located 40 bp upstream of the *sqr* start codon (Fig. S1).

Wild-type (WT) *R. capsulatus* cells cannot grow with lactose as a sole carbon source, because *R. capsulatus* does not encode the

Fig. 1. Sulfide responsiveness of the *sqr* promoter regions. (*A*) β-Galactosidase activity measurements of the *sqr* promoter region of 1,238 bp upstream of the start codon and *lacZ* fusion. Cells were grown to midlog phase under aerobic conditions and 0.6 mM Na₂S (triangles) or nothing (squares) was added at *t* = 0. Cells were harvested at each time point and assayed for β-galactosidase activity. Error bars indicate SD of the mean. ONP, *o*-nitrophenyl-β-D-galactopyranoside. (*B*) Same as in *A*, except that cells were grown under anaerobic conditions.

lac operon in its genome. However, *R. capsulatus* containing the *sqr::lacZ* fusion construct can grow on lactose-containing medium in the presence of sulfide but not in the absence of sulfide. This sulfide-dependent growth allowed the screening of sulfide-insensitive suppressor mutants. Specifically, *R. capsulatus* expressing the full-length *sqr::lacZ* gene fusion was treated with ethyl methanesulfonate to induce point mutations, with these mutagenized cells plated onto lactose plates for selective growth under aerobic conditions in the absence of sulfide. From this selection, we isolated ~30 colonies from 10^8 mutagenized cells that exhibited growth independent of the presence of sulfide (Fig. S2*A*). We sequenced the reporter plasmids from these strains to confirm that there were no mutations present in the *sqr* promoter region, and then applied genome sequence analysis to identify suppressor mutations. Genomic suppressor mutations in several candidate genes were found (Dataset S1). Disruption of one candidate gene, which we named sulfide:quinone reductase repressor (*sqrR*) (GenBank accession no. ADE85198), yielded constitutively high *sqr* expression even in the absence of sulfide, suggesting that it likely encodes a transcriptional repressor (Fig. S2*B*). Oxidative stress resulting from H_2O_2 treatment does not significantly affect *sqr* expression in the WT or the *sqrR* mutant strain (Fig. S3*A*), with the *sqrR* gene constitutively expressed, although at a level slightly decreased by sulfide treatment (Fig. S3*B*). *R. capsulatus* encodes two homologs of the previously characterized homotetrameric persulfide sensor from *S. aureus*, CstR (26), and deletion strains of one or both *cstR*-like genes are fully sulfide-responsive (Fig. S2*C*). These two CstR paralogs are most closely related to the formaldehyde-sensing repressor FrmR (GenBank accession no. ADE84633) and the nickel-sensing repressor RcnR (GenBank accession no. ADE83853) (Fig. S4*A*), and are structurally unrelated to SqrR (28, 29). These data taken collectively reveal that SqrR is the primary sulfide sensor in *R. capsulatus*.

There are two possible AUG initiation codons separated by 13 residues in the putative *sqrR* ORF. To determine the exact start codon for SqrR translation, translational *lacZ* fusions to each start codon were constructed with subsequent β-galactosidase activity measurements; these experiments reveal that the more downstream initiation codon is the bona fide start of translation (Fig. S5). A bioinformatics analysis reveals that SqrR homologs are present in nearly all major classes of proteobacteria. A multiple-amino acid sequence alignment of SqrR homologs from α-, β-, and γ-proteobacteria reveals several conserved regions, including the helix-turn-helix motif and two highly conserved cysteines (Fig. S4*B*). SqrR is a member of the arsenic repressor (ArsR) family of prokaryotic repressors (30), and is evolutionarily related to BigR from the plant pathogens *Xyella* and *Agrobacterium* spp., described previously as mediating hydrogen sulfide detoxification (31). An unrooted phylogenetic tree of SqrR homologs indicates that some β- and γ-proteobacterial SqrR homologs are found within the α-proteobacterial clade, suggesting lateral gene transfer of *sqrR* among proteobacteria (Fig. S4*C*).

Biochemical Properties of SqrR. We next purified recombinant *R. capsulatus* SqrR for in vitro studies using an *Escherichia coli* overexpression system followed by affinity chromatography. DNase I footprint analysis was undertaken with purified SqrR to determine the site of SqrR binding to the *sqr* promoter region (Fig. 2*A*). Good protection was observed in the *sqr* promoter region around the −10 σ-subunit recognition sequences and transcriptional start site, consistent with the classification of SqrR as a transcriptional repressor. Gel mobility-shift analysis of purified SqrR was next carried out with a DNA probe that encompasses the SqrR-protected region in the *sqr* promoter. These assays were performed with untreated and fully reduced SqrR as well as with SqrR treated with a representative persulfide sulfur donor, GSSH. To avoid oxidation of Cys residues by molecular oxygen, all
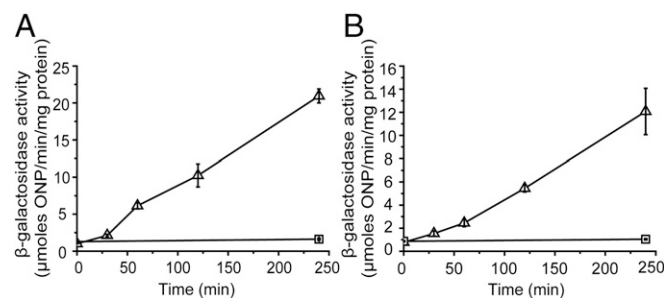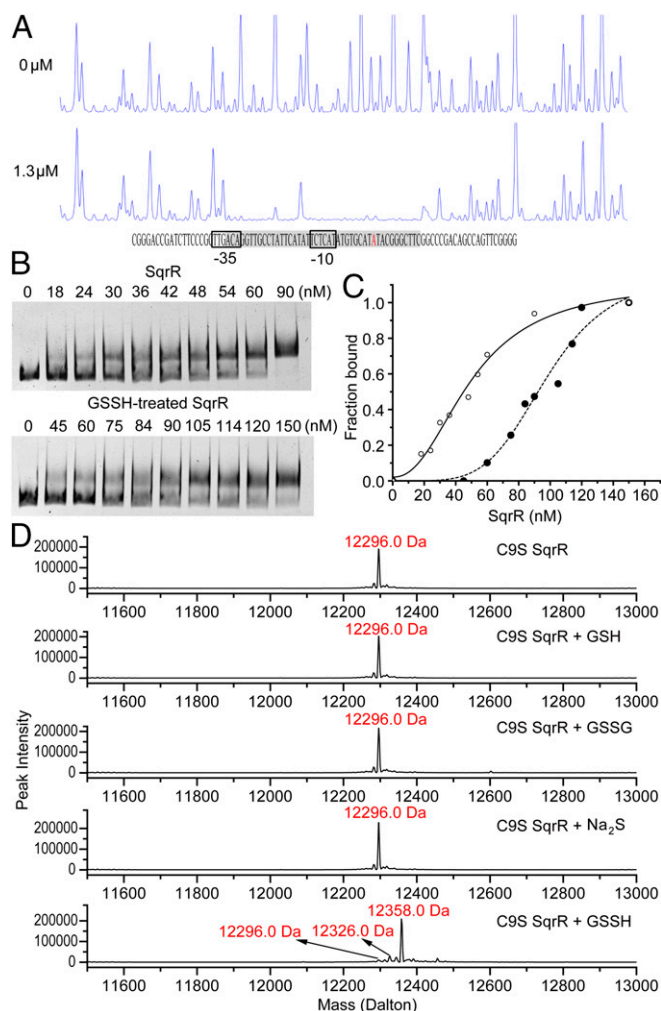
Fig. 2. Biochemical properties of SqrR. (*A*) DNase I footprint analysis of SqrR. Binding to the *sqr* promoter region under aerobic conditions. (*A*, *Bottom*) Regions corresponding to the DNase I protection regions are shown with a gray background. The −35 and −10 σ-subunit recognition sequences are in boxed letters, with the transcription start site indicated in red. (*B*) Gel mobility-shift assay using a DNA fragment of the *sqr* promoter region under anaerobic conditions with reduced SqrR (18 to 90 nM) or GSSH-treated SqrR (45 to 150 nM). (*C*) Binding isotherms of reduced (open circles and solid line) and GSSH-treated SqrR (filled circles and dashed line) plotted as a fraction of the shifted probe. (*D*) C9S SqrR reacts with glutathione persulfide but not glutathione, glutathione disulfide, or Na$_2$S to form intramolecular cross-links. LC-ESI-MS spectra of reduced C9S SqrR, GSH-reacted C9S SqrR, GSSG-reacted C9S SqrR, Na$_2$S-reacted C9S SqrR, and GSSH-reacted C9S SqrR. Monomeric C9S SqrR (12,296 Da) was found to be the dominant species in all samples except for GSSH-reacted C9S SqrR, in which the tetrasulfide–cross-linked C9S SqrR (12,358 Da) was found to dominate, accompanied by a small amount (≤5%) of trisulfide–cross-linked C9S SqrR (12,326 Da). Conditions: 25 mM Tris·HCl, 200 mM NaCl, 2 mM EDTA (pH 8.0).

experiments were carried out under anaerobic conditions. SqrR binds to the DNA probe in a concentration-dependent manner (Fig. 2*B*), yielding an EC$_{50}$ value (effective concentration of SqrR for 50% binding) (Fig. 2*C*) for untreated (reduced) SqrR of ∼56 nM, which is approximately twofold lower than that of GSSH-treated SqrR (∼110 nM). The DNA-binding affinity of untreated and fully reduced C9S SqrR is significantly higher than that of GSSH-treated C9S SqrR, suggesting that C9S SqrR, like WT SqrR, is fully capable of sensing persulfides (Fig. S6*A*). In striking contrast, the C41S and C107S SqrRs do not show a significant GSSH-dependent reduction in DNA affinity, with EC$_{50}$ values

(∼50 nM) similar to that of WT reduced SqrR (Fig. S6 *B* and *C*). Finally, aerobic gel mobility-shift experiments carried out in the absence or presence of the reductant DTT reveal that the affinity of SqrR is significantly higher in the presence of DTT relative to its absence (Fig. S6*D*). These experiments collectively reveal that the operator-promoter DNA-binding affinity of SqrR in vitro is sensitive to reversible thiol oxidation such as disulfide-bond formation, as previously observed for the SqrR homolog BigR (31).

To define the chemical nature of the SqrR modification by GSSH, we measured the molecular mass distribution of C9S SqrR species following an anaerobic incubation with an excess of GSSH by liquid chromatography (LC) coupled with a mass spectrometer (MS) equipped with an electrospray interface (ESI). These mass spectra were compared with those obtained with untreated, reduced SqrR vs. those incubated with the corresponding thiol, glutathione (GSH), glutathione disulfide (GSSG), and Na$_2$S (Fig. 2*D*). C9S SqrR is active in cells (*vide infra*), and was used for these experiments to minimize complications from oxidative chemistry occurring at Cys9. We find that untreated C9S SqrR is fully reduced, with no evidence of other modifications (M_r 12,296 Da). We observe no change in this mass spectrum in the presence of GSH, GSSG, or Na$_2$S. In contrast, GSSH specifically shifts the mass distribution to that largely corresponding to a +62-Da species, a mass shift consistent with an intramolecular (intraprotomer) tetrasulfide cross-link between the remaining C41 and C107 residues (Fig. 2*D*). In addition, a small amount of +30-Da product is also observed, consistent with an intramolecular trisulfide cross-link (Fig. 2*D*). High-resolution tandem mass spectrometry of trypsin-digested GSSH-treated C9S SqrR confirms the presence of both intramolecular tri- and tetrasulfide cross-links linking C41 and C107 on the same subunit (Fig. S7).

Similar findings were obtained for the WT SqrR. Specifically, incubation with GSSH, but not GSH, GSSG, and Na$_2$S, results in molecular mass shifts of +30 and +62 Da, with the latter the major product (Fig. S8*A*), consistent with intramolecular tri- and tetrasulfide cross-links between C41 and C107, as described for C9S SqrR. Tandem ESI-MS/MS analysis of the trisulfide–cross-linked species confirms this assignment in the +3 charge state (Fig. S8*B*). Both cross-links are fully reduced by the thiol-reducing agent Tris (2-carboxyethyl)phosphine (TCEP) (Fig. S8*A*), establishing the reversibility of the tri- and tetrasulfide bonds in SqrR. Interestingly, a number of *S*-glutathionylated adducts were also observed in GSSG- and GSSH-derivatized WT SqrR relative to C9S SqrR (Fig. S8*C*), but the significance of this *S*-glutathionylation is unknown, because C9S SqrR is fully functional in cells (*vide infra*). Intraprotomer cross-linking between C41 and C107 is supported by a model structure of SqrR derived from crystal structures of *Xylella fastidiosa* BigR, an SqrR homolog, in the disulfide-oxidized and thiol-reduced states (32) (Fig. 3*A*). Oxidized BigR is characterized by an intramolecular disulfide bond between two cysteines that correspond to C41 and C107 in *R. capsulatus* SqrR (31). These two cysteine residues must be in close physical proximity, as would be required for intramolecular di-, tri-, and tetrasulfide-bond formation in SqrR.

We next constructed strains of *R. capsulatus* where each SqrR cysteine (C9, C41, and C107) was individually changed to a serine and recombined into its native genomic locus to determine the degree to which these residues impact the ability of SqrR to sense exogenous sulfide in vivo. As expected, the C41S and C107S mutants both lose the ability to derepress *sqr* expression in the presence of exogenous sulfide; in contrast, the C9S mutant retains WT transcriptional derepression activity (Fig. 3*B*). The C41S mutant was impaired in photoautotrophic growth using H$_2$S as a sole electron donor (Fig. S9*A*), and Δ*sqrR* and C41S mutants exhibited a more pale or a darker color, respectively, than the WT strain on a sulfide-containing growth medium (Fig. S9*B*). Under these conditions, bacteriochlorophyll and carotenoid contents in the Δ*sqrR* strain were ∼30% lower than in WT. Photosynthetic
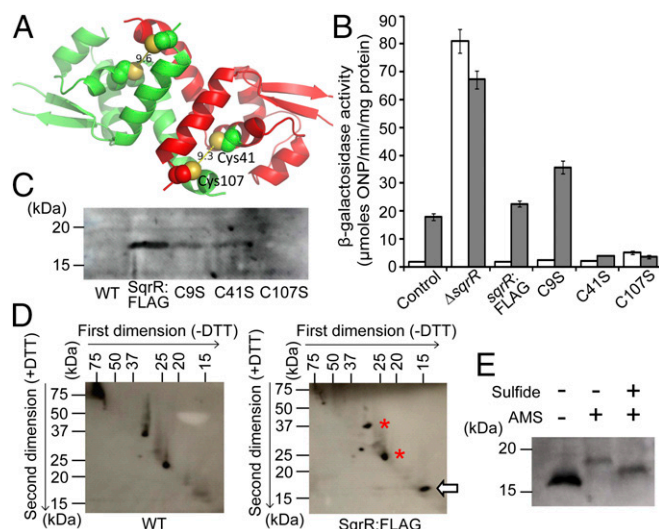
Fig. 3. Characterization of SqrR in vivo. (*A*) Structural model of SqrR based on the structure of *Xylella* BigR (32). Red and green are used to distinguish the two subunits (protomers) of the homodimer. Yellow spheres highlight the two cysteines (C41 and C107) separated by ~9.5 Å in this model. (*B*) β-Galactosidase activity measurements are as in Fig. 1. The control is the WT strain containing the *sqr–lacZ* fusion. Aerobically grown cells that reached midlog phase were induced by sodium sulfide (gray bars) or not induced (open bars), and then cells were harvested after 4 h. A FLAG-tagged coding sequence was integrated into the genomic *sqrR* 3′ end in *R. capsulatus* (SqrR:FLAG). Each point mutant was constructed using the *sqrR*-FLAG mutant as background. Error bars indicate SD of the mean. (*C*) Detection of C-terminally FLAG-tagged WT and mutant SqrRs by Western blotting using an anti-FLAG antibody. (*D*) Nonreducing (–DTT) and reducing (+DTT) 2D electrophoresis coupled with Western blotting using an anti-FLAG antibody. WT (negative control) and SqrR-FLAG strains grown aerobically were treated with 0.6 mM Na₂S for 4 h and then subjected to SDS/PAGE. An arrow indicates the specific band for the SqrR-FLAG monomer. Red asterisks indicate nonspecific bands. (*E*) Mobility shifts of SqrR caused by thiol modification on SDS/polyacrylamide gels. The SqrR-FLAG mutant was labeled with AMS. Cells were grown to midlog phase under aerobic conditions, followed by the addition of 0.6 mM sodium sulfide. Before harvesting, cells were treated with trichloroacetic acid (TCA) to rapidly quench thiol–disulfide exchange reactions.

growth profiles of WT and Δ*sqrR* were also analyzed. Cells precultured in the presence and absence of sulfide were transferred to sulfide-free fresh medium and growth rates were measured under anaerobic light conditions (Fig. S9C). When cells were transferred from sulfide-containing medium to sulfide-free medium, slow growth was observed before the logarithmic growth phase, although such delayed growth was not observed when cells were transferred from sulfide-free preculture. Notably, the delayed growth phenotype of Δ*sqrR* was longer (~8 h) than that of WT (~4 h). These experiments establish the physiological importance of the tetrasulfide-bond formation of SqrR for sulfide utilization and regulated photopigment synthesis.

To assess the stability of mutant SqrRs in cells, we performed Western blot analysis using C-terminally FLAG-tagged SqrRs and an anti-FLAG antibody. Given that the FLAG tag was integrated into the *sqrR* 3′-end coding sequence, the copy numbers should be similar to those of the WT. WT SqrR-FLAG could be specifically detected, with both C9S and C41S SqrRs also detected, albeit at levels modestly lower than WT SqrR (Fig. 3C). Although C107S SqrR was not detected in this experiment, this may be due to a lower stability and/or loss of the FLAG tag, because the *sqr* repressor activity of C107S SqrR is only modestly affected and readily distinguished from a Δ*sqrR* strain (Fig. S2D). Two-dimensional nonreducing and reducing electrophoresis coupled with Western blot detection reveals that SqrR does not form covalently cross-

linked dimers in cells in the presence of sulfide stress (Fig. 3D), a finding consistent with the the in vitro mass spectrometry experiments indicative of an intraprotomer cross-link (Fig. 2D and Fig. S8). To confirm the presence of an intraprotomer C41–C107 cross-link, total protein extracts were treated with the thiol-modifying agent 4-acetamido-4′-maleimidylstilbene-2,2′-disulfonic acid (AMS), which derivatizes only free Cys sulfhydryl groups, followed by analysis by SDS/PAGE and Western blotting. A tetrasulfide bond would be resistant to AMS modification, so any AMS modifications that retard electrophoretic mobility would reflect the status of free Cys sulfhydryls in SqrR. As shown in Fig. 3E, the molecular mass of SqrR-FLAG in non–sulfide-treated vs. sulfide-treated cells is increased by ~2.4 and ~0.8 kDa, respectively, after treatment with AMS relative to that of SqrR-FLAG that was not modified with AMS. Given that the increase in molecular mass of the non–sulfide-treated sample is approximately threefold that of the sulfide-treated sample, we conclude that the number of free Cys sulfhydryls is changed from three to one after treatment of cells with exogenous sulfide. Although the nature of the C41–C107 cross-link in SqrR isolated from cells can be defined by this experiment, these findings are fully consistent with the in vitro GSSH–cross-linking experiments (Fig. 2 and Fig. S8) in that there are two cysteine residues of SqrR that are cross-linked by exogenous sulfide-derived reactive sulfur species in vivo.

Identification of Genes Controlled by SqrR. To identify SqrR-regulated genes, we performed an RNA-sequencing (RNA-seq) transcriptomic analysis of the *R. capsulatus* WT and *sqrR*-disrupted mutant in the absence and presence of exogenous sulfide. In one experiment, we identified sulfide-inducible genes in WT cells by comparing transcription levels in WT cells untreated vs. treated with sulfide. In a parallel experiment, we identified SqrR-regulated genes by comparing the expression levels in WT vs. *sqrR* mutant cells grown in the absence of sulfide (Dataset S2). These results reveal that 45% of all sulfide-responsive genes in the *R. capsulatus* genome are directly or indirectly regulated by SqrR. The identified sulfide-responsive genes include a number of genes known to function in sulfur metabolism or assimilation, including thiosulfate-sulfite oxidoreductases and thiosulfate sulfurtransferases or rhodanese homology domain proteins (33, 34), whose expression is strongly repressed by SqrR. Although originally described as functioning in cyanide detoxification (35), sulfurtransferases and structurally unrelated single-Cys–containing TusA domains (36) are generally involved in persulfide shuttling, and are capable of accepting sulfur from a variety of RSS, including thiosulfate and low-molecular-weight persulfides (37). Another major target of SqrR is a putative peroxiredoxin, a thiol peroxidase known to be involved in detoxification of reactive oxygen species (38); this finding suggests a novel role in detoxification of RSS. Interestingly, the expression of diguanylate cyclase/phosphodiesterase, which catalyzes bis-(3′-5′)-cyclic dimeric guanosine monophosphate (c-di-GMP) synthesis, and acetone carboxylase are also regulated by SqrR. A divergently transcribed operon encoding an RND family efflux transporter and acriflavin resistance protein located downstream of *sqrR* are also strongly repressed by SqrR. Although the repression level is not high, sulfite assimilation- and cysteine biosynthesis-related genes are also regulated by SqrR. Comparison of the promoter sequences of genes characterized by ≥10-fold changes by *sqrR* disruption reveals a strong consensus operator sequence for SqrR, namely ATTC-N₈-GAAT (Fig. S10). Interestingly, the expression of most genes in the photosynthetic gene cluster (*puf, puc, bch,* and *crt*) are ~0.5-fold repressed in the *sqrR* mutant relative to WT cells.

Discussion

In this study, we have identified and characterized a novel sulfide-responsive transcriptional repressor, SqrR, that controls sulfide-dependent photosynthetic electron transfer in *R. capsulatus*. The
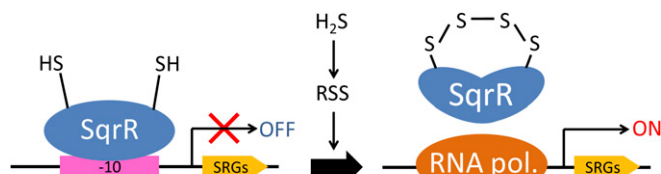
Fig. 4. Model for SqrR sulfide-responsive gene regulation. In the absence of hydrogen sulfide, C41 and C107 of SqrR are in the reduced form. This form of SqrR binds the promoter region and represses the expression of sulfide-responsive genes (SRGs). In the presence of hydrogen sulfide, the resultant cellular RSS promotes the formation of a di-, tri-, or tetrasulfide bond between C41 and C107, inhibiting the ability of SqrR to bind to the promoter region. RNA polymerase binds DNA and subsequently induces gene expression.

expression level of *sqr*, which encodes a canonical sulfide:quinone oxidoreductase (39, 40), is induced by sulfide in WT cells and is elevated in the *sqrR*-disrupted mutant irrespective of the presence of sulfide (Fig. 3B). The DNA-binding activity of purified SqrR is significantly reduced upon anaerobic incubation of GSSH, revealing that negative regulation of DNA binding and transcriptional derepression in cells involves thiol modifications (Fig. 2C). Two cysteine residues, at positions 41 and 107, are conserved in SqrR homologs from other bacteria, and substitution of each with serine results in the loss of a GSSH-responsive decrease in DNA-binding affinity in vitro (Fig. S6 B and C) and sulfide-dependent regulation in vivo (Fig. 3B). LC-ESI-MS/MS analysis shows that GSSH reacts with purified and fully reduced WT and C9S SqrRs to increase the molecular mass by +30 or +62 Da, with the latter species predominating (Fig. 2D and Fig. S8A). Furthermore, in sulfide-treated relative to untreated cells, SqrR harbors two cysteine residues that cannot be modified by AMS (Fig. 3E). Our data collectively reveal that C41 and C107 form an intramolecular tetrasulfide bond upon sensing of sulfide-derived reactive sulfur species, such as glutathione persulfide, that are expected to accumulate in sulfide-treated bacterial cells (39) (Fig. 4).

It was previously shown that the SqrR homolog BigR from *X. fastidiosa* is capable of forming an intramolecular disulfide bond in vitro via an unknown mechanism but that formation of this disulfide was proposed to be important in the detoxification of hydrogen sulfide, specifically under hypoxic, biofilm-promoting conditions (31). Here we show that purified *R. capsulatus* SqrR also forms an intramolecular di-, tri-, or tetrasulfide bond, which we show reduces its DNA-binding affinity in vitro (Fig. S6D). Consistent with a role in sensing reactive sulfur species rather than reactive oxygen species, SqrR-dependent transcriptional regulation in vivo is specifically sulfide-inducible and independent of oxygen and/or redox status of the cell (Fig. 1 and Fig. S3A). The findings parallel those previously described for the persulfide sensor CstR from *S. aureus* (26). These results reveal that SqrR in *R. capsulatus* senses sulfide and is not a simple redox sensor. The difference between SqrR and BigR functions may be due to their distinct metabolic features, as *R. capsulatus* is a facultative anaerobic bacterium whereas *X. fastidiosa* is strictly aerobic.

SqrR is a member of the ArsR family of bacterial repressors encoding a wide range of metal-, metalloid-, and non–metal-sensing proteins (41, 42). This structural classification contrasts sharply with that of the only other known sulfide-responsive, persulfide-sensing repressor, CstR, from *S. aureus*, which is a member of the CsoR/RcnR family of metalloregulatory proteins (43). Homotetrameric CstR forms intersubunit di-, tri-, and tetrasulfide bonds between two conserved cysteines in the presence of low-molecular-weight persulfides and inorganic polysulfides that negatively regulate DNA-binding affinity to target promoters in sulfide-stressed cells (26). Although *R. capsulatus* harbors two CstR-like proteins, they are true paralogs predicted to function in formaldehyde detoxification (FrmR) (29) and nickel homeostasis (RcnR) (Fig. S4A).

Consistent with this, deletion of either or both genes in *R. capsulatus* has no effect on *sqr* expression (Fig. S2C). Our RNA-seq analysis indicates that SqrR contributes to the regulation of many (45%) of the sulfide-responsive genes. These SqrR-regulated genes include not only those anticipated RSS detoxification proteins and persulfide carriers but also c-di-GMP cyclase/phosphodiesterase and acetone carboxylase. C-di-GMP, known as a bacterial second messenger, affected sulfide homeostasis to motility and biofilm formation in *X. fastidiosa* (31); furthermore, the electrophilic C8 position of guanine nucleotides is reported to be a significant site of thiolation by RSS in mammalian cells (13). Acetone carboxylase, on the other hand, is involved in nonrubisco CO_2 fixation (44), and may therefore function as an inducible electron sink. SqrR also regulates RND family efflux transporter genes, suggesting a role in reductase assembly. Furthermore, genes that show a ≥8-fold sulfide-dependent change in expression are clearly regulated by SqrR. Based on these observations, we conclude that SqrR is the master regulator of sulfide response in *R. capsulatus*.

Disruption of *sqrR* also influences the expression of photosynthesis-related genes in the photosynthesis gene cluster. The expression changes may be due to alteration of the redox status of the quinone pool, which would influence the phosphorylation activity of the sensor kinase RegB, known to control photosynthesis gene expression in response to alterations in the ubiquinone pool (45). These observations suggest that regulating the synthesis of the photosynthetic apparatus involves the synchronization of electron transfer activities among several components, with expression responding to different electron donors that are variable in nature. A non–sulfide-responsive mutant SqrR impacts sulfide-dependent pigmentation (Fig. S9), consistent with this hypothesis.

In mammalian cells, a small but significant fraction of the proteome is persulfidated as a result of the endogenous production of H_2S by enzymes of the transsulfuration pathway, which potentially results in significant metabolic changes in the cell (18). The extent to which such intramolecular signaling by RSS and shifts in metabolism are operative in bacteria is currently unknown. These studies establish that the sulfide-regulated repressor SqrR allows *R. capsulatus* to adapt to changes in sulfide availability via thiol persulfidation chemistry on SqrR, which we hypothesize involves the intermediacy of RSS in cells. The functional characteristics of SqrR appear largely analogous to those of CstR in *S. aureus* (26), which also regulates an H_2S oxidation and detoxification system (46), despite vastly distinct structural scaffolds (47). Further elucidation of the functional role(s) of persulfide trafficking and sulfide homeostasis in *R. capsulatus* promises a better understanding of how these processes impact photosynthesis in this industrially important bacterium.

Materials and Methods

Materials and methods are described in *SI Materials and Methods*. They include bacterial strains, growth conditions, mutagenesis, genetic sulfide-insensitive suppressor mutant screening, purification of recombinant SqrR, primer extension analysis, GSSH preparation, LC-ESI-MS analysis, LC-MS/MS analysis, gel mobility-shift analysis, DNase I footprint assay, β-galactosidase assay, Western blotting, extraction of photosynthetic pigments, and RNA-seq.

Data represent the mean of at least three independent experiments (error bars indicate SD of the mean). The P value and statistical significance of difference were analyzed by using unpaired t tests ($P < 0.05$, significant).

MICROBIOLOGY

1. Godet L, Zelnio KA, Van Dover CL (2011) Scientists as stakeholders in conservation of hydrothermal vents. *Conserv Biol* 25(2):214–222.
2. Baross JA, Hoffman SE (1985) Submarine hydrothermal vents and associated gradient environments as sites for the origin and evolution of life. *Orig Life Evol Biosph* 15(4): 327–345.
3. Corliss JB, Baross JA, Hoffman SE (1981) An hypothesis concerning the relationship between submarine hot springs and the origin of life on Earth. *Oceanol Acta* 1980: 59–69.
4. Ishibashi J, Okino K, Sunamura M, eds (2015) *Subseafloor Biosphere Linked to Hydrothermal Systems: TAIGA Concept* (Springer, Tokyo).
5. Fisher C, Takai K, Le Bris N (2007) Hydrothermal vent ecosystems. *Oceanography* 20(1): 14–23.
6. Beatty JT, et al. (2005) An obligately photosynthetic bacterial anaerobe from a deep-sea hydrothermal vent. *Proc Natl Acad Sci USA* 102(26):9306–9310.
7. Bauer C, Elsen S, Swem LR, Swem DL, Masuda S (2003) Redox and light regulation of gene expression in photosynthetic prokaryotes. *Philos Trans R Soc Lond B Biol Sci* 358(1429):147–153. discussion 153–154.
8. Zeilstra-Ryalls JH, Kaplan S (2004) Oxygen intervention in the regulation of gene expression: The photosynthetic bacterial paradigm. *Cell Mol Life Sci* 61(4):417–436.
9. Kaneko Y, Kimura Y, Kimura H, Niki I (2006) L-cysteine inhibits insulin release from the pancreatic beta-cell: Possible involvement of metabolic production of hydrogen sulfide, a novel gasotransmitter. *Diabetes* 55(5):1391–1397.
10. Kimura H (2010) Hydrogen sulfide: From brain to gut. *Antioxid Redox Signal* 12(9): 1111–1123.
11. Wang R (2012) Physiological implications of hydrogen sulfide: A whiff exploration that blossomed. *Physiol Rev* 92(2):791–896.
12. Zhang D, et al. (2014) Detection of protein *S*-sulfhydration by a tag-switch technique. *Angew Chem Int Ed Engl* 53(2):575–581.
13. Ida T, et al. (2014) Reactive cysteine persulfides and *S*-polythiolation regulate oxidative stress and redox signaling. *Proc Natl Acad Sci USA* 111(21):7606–7611.
14. Nishida M, et al. (2012) Hydrogen sulfide anion regulates redox signaling via electrophile sulfhydration. *Nat Chem Biol* 8(8):714–724.
15. Cuevasanta E, et al. (2015) Reaction of hydrogen sulfide with disulfide and sulfenic acid to form the strongly nucleophilic persulfide. *J Biol Chem* 290(45):26866–26880.
16. Yadav PK, et al. (2016) Biosynthesis and reactivity of cysteine persulfides in signaling. *J Am Chem Soc* 138(1):289–299.
17. Mustafa AK, et al. (2009) H_2S signals through protein *S*-sulfhydration. *Sci Signal* 2(96): ra72.
18. Gao XH, et al. (2015) Quantitative H_2S-mediated protein sulfhydration reveals metabolic reprogramming during the integrated stress response. *eLife* 4:e10067.
19. Dóka É, et al. (2016) A novel persulfide detection method reveals protein persulfide- and polysulfide-reducing functions of thioredoxin and glutathione systems. *Sci Adv* 2(1):e1500968.
20. Wedmann R, et al. (2016) Improved tag-switch method reveals that thioredoxin acts as depersulfidase and controls the intracellular levels of protein persulfidation. *Chem Sci (Camb)* 7(5):3414–3426.
21. Cooper CE, Brown GC (2008) The inhibition of mitochondrial cytochrome oxidase by the gases carbon monoxide, nitric oxide, hydrogen cyanide and hydrogen sulfide: Chemical mechanism and physiological significance. *J Bioenerg Biomembr* 40(5): 533–539.
22. Meyer TE, Cusanovich MA (2003) Discovery and characterization of electron transfer proteins in the photosynthetic bacteria. *Photosynth Res* 76(1–3):111–126.
23. Gregersen LH, Bryant DA, Frigaard N-U (2011) Mechanisms and evolution of oxidative sulfur metabolism in green sulfur bacteria. *Front Microbiol* 2:116.
24. Libiad M, Yadav PK, Vitvitsky V, Martinov M, Banerjee R (2014) Organization of the human mitochondrial hydrogen sulfide oxidation pathway. *J Biol Chem* 289(45): 30901–30910.
25. Griesbeck C, et al. (2002) Mechanism of sulfide-quinone reductase investigated using site-directed mutagenesis and sulfur analysis. *Biochemistry* 41(39):11552–11565.
26. Luebke JL, et al. (2014) The CsoR-like sulfurtransferase repressor (CstR) is a persulfide sensor in *Staphylococcus aureus*. *Mol Microbiol* 94(6):1343–1360.
27. Sganga MW, Bauer CE (1992) Regulatory factors controlling photosynthetic reaction center and light-harvesting gene expression in *Rhodobacter capsulatus*. *Cell* 68(5): 945–954.
28. Higgins KA, Giedroc D (2014) Insights into protein allostery in the CsoR/RcnR family of transcriptional repressors. *Chem Lett* 43(1):20–25.
29. Osman D, et al. (2016) The effectors and sensory sites of formaldehyde-responsive regulator FrmR and metal-sensing variant. *J Biol Chem* 291(37):19502–19516.
30. Ma Z, Jacobsen FE, Giedroc DP (2009) Coordination chemistry of bacterial metal transport and sensing. *Chem Rev* 109(10):4644–4681.
31. Guimarães BG, et al. (2011) Plant pathogenic bacteria utilize biofilm growth-associated repressor (BigR), a novel winged-helix redox switch, to control hydrogen sulfide detoxification under hypoxia. *J Biol Chem* 286(29):26148–26157.
32. Barbosa RL, Rinaldi FC, Guimarães BG, Benedetti CE (2007) Crystallization and preliminary X-ray analysis of BigR, a transcription repressor from *Xylella fastidiosa* involved in biofilm formation. *Acta Crystallogr Sect F Struct Biol Cryst Commun* 63(Pt 7): 596–598.
33. Higgins KA, Peng H, Luebke JL, Chang FMJ, Giedroc DP (2015) Conformational analysis and chemical reactivity of the multidomain sulfurtransferase, *Staphylococcus aureus* CstA. *Biochemistry* 54(14):2385–2398.
34. Cipollone R, Ascenzi P, Visca P (2007) Common themes and variations in the rhodanese superfamily. *IUBMB Life* 59(1):51–59.
35. Roy AB, Trudinger PA (2010) *The Biochemistry of Inorganic Compounds of Sulphur* (Cambridge Univ Press, Cambridge, United Kingdom).
36. Shi R, et al. (2010) Structural basis for Fe-S cluster assembly and tRNA thiolation mediated by IscS protein-protein interactions. *PLoS Biol* 8(4):e1000354.
37. Mueller EG (2006) Trafficking in persulfides: Delivering sulfur in biosynthetic pathways. *Nat Chem Biol* 2(4):185–194.
38. Perkins A, Poole LB, Karplus PA (2014) Tuning of peroxiredoxin catalysis for various physiological roles. *Biochemistry* 53(49):7693–7705.
39. Shen J, Peng H, Zhang Y, Trinidad JC, Giedroc DP (2016) *Staphylococcus aureus* sqr encodes a type II sulfide:quinone oxidoreductase and impacts reactive sulfur speciation in cells. *Biochemistry* 55(47):6524–6534.
40. Marcia M, Ermler U, Peng G, Michel H (2010) A new structure-based classification of sulfide:quinone oxidoreductases. *Proteins* 78(5):1073–1083.
41. Busenlehner LS, Pennella MA, Giedroc DP (2003) The SmtB/ArsR family of metalloregulatory transcriptional repressors: Structural insights into prokaryotic metal resistance. *FEMS Microbiol Rev* 27(2–3):131–143.
42. Campbell DR, et al. (2007) Mycobacterial cells have dual nickel-cobalt sensors: Sequence relationships and metal sites of metal-responsive repressors are not congruent. *J Biol Chem* 282(44):32298–32310.
43. Chang FMJ, et al. (2014) Cu(I)-mediated allosteric switching in a copper-sensing operon repressor (CsoR). *J Biol Chem* 289(27):19204–19217.
44. Birks SJ, Kelly DJ (1997) Assay and properties of acetone carboxylase, a novel enzyme involved in acetone-dependent growth and CO_2 fixation in *Rhodobacter capsulatus* and other photosynthetic and denitrifying bacteria. *Microbiology* 143:755–766.
45. Wu J, Bauer CE (2008) RegB/RegA, a global redox-responding two-component system. *Adv Exp Med Biol* 631:131–148.
46. Shen J, et al. (2015) *Staphylococcus aureus* CstB is a novel multidomain persulfide dioxygenase-sulfurtransferase involved in hydrogen sulfide detoxification. *Biochemistry* 54(29):4542–4554.
47. Chaturvedi KS, et al. (2014) Cupric yersiniabactin is a virulence-associated superoxide dismutase mimic. *ACS Chem Biol* 9(2):551–561.
48. Shimizu T, Cheng Z, Matsuura K, Masuda S, Bauer CE (2015) Evidence that altered *cis* element spacing affects PpsR mediated redox control of photosynthesis gene expression in *Rubrivivax gelatinosus*. *PLoS One* 10(6):e0128446.
49. Young DA, Bauer CE, Williams JC, Marrs BL (1989) Genetic evidence for superoperonal organization of genes for photosynthetic pigments and pigment-binding proteins in *Rhodobacter capsulatus*. *Mol Gen Genet* 218(1):1–12.
50. Zeller T, et al. (2007) Regulation of hydrogen peroxide-dependent gene expression in *Rhodobacter sphaeroides*: Regulatory functions of OxyR. *J Bacteriol* 189(10): 3784–3792.
51. Li H, Durbin R (2009) Fast and accurate short read alignment with Burrows-Wheeler transform. *Bioinformatics* 25(14):1754–1760.
52. Li H, et al.; 1000 Genome Project Data Processing Subgroup (2009) The Sequence Alignment/Map format and SAMtools. *Bioinformatics* 25(16):2078–2079.
53. Masuda S, Bauer CE (2004) Null mutation of HvrA compensates for loss of an essential relA/spoT-like gene in *Rhodobacter capsulatus*. *J Bacteriol* 186(1):235–239.
54. Jiang ZY, Gest H, Bauer CE (1997) Chemosensory and photosensory perception in purple photosynthetic bacteria utilize common signal transduction components. *J Bacteriol* 179(18):5720–5727.
55. Thompson JD, Gibson TJ, Plewniak F, Jeanmougin F, Higgins DG (1997) The CLUSTAL_X windows interface: Flexible strategies for multiple sequence alignment aided by quality analysis tools. *Nucleic Acids Res* 25(24):4876–4882.
56. Kumar S, Tamura K, Nei M (2004) MEGA3: Integrated software for molecular evolutionary genetics analysis and sequence alignment. *Brief Bioinform* 5(2):150–163.